AFTERMATH OF THE END-CRETACEOUS MASS EXTINCTION: POSSIBLE BIOGEOCHEMICAL STABILIZATION OF THE CARBON CYCLE AND CLIMATE

Ken Caldeira[1]

Earth System Science Center, Pennsylvania State University, University Park

Michael R. Rampino

Department of Earth System Science, New York University, New York

Abstract. In the aftermath of the Cretaceous/ Tertiary (K/T) boundary event (~65 m.y. ago), pelagic carbonate productivity was greatly reduced for several hundred thousand years. A decrease in carbonate productivity by a factor greater than 3, in the absence of some mechanism to remove excess carbonate from the ocean, should have resulted in the accumulation of carbon and alkalinity in the oceans. This would cause the atmospheric partial pressure of CO_2 to fall dramatically and the deep ocean to become fully saturated with respect to calcite. Evidence of such a period of highly calcite-saturated oceans with low atmospheric pCO_2 in the earliest Tertiary is lacking, suggesting that ocean chemistry may have been buffered by some process or processes. Shallow-water carbonate accumulation rates may depend, in part, on carbonate ion concentrations, and thus shallow-water carbonate deposition might act to stabilize ocean chemistry in the face of a dramatic reduction in pelagic productivity. In our four-box ocean model, as the oceanic carbonate ion concentration rises in the face of diminished pelagic carbonate accumulation, the shallow-water carbonate accumulation rate increases, compensating for the reduction in pelagic carbonate accumulation. These model results indicate that the carbonate-ion feedback on shallow-water carbonate sedimentation may have acted to balance oceanic carbon and alkalinity budgets at the K/T boundary, and, furthermore, may have been a primary mechanism maintaining high shallow-water carbonate accumulation rates prior to the Jurassic onset of widespread pelagic carbonate accumulation.

INTRODUCTION

The primary sources of carbon dioxide to the oceans and atmosphere are the chemical weathering of carbonate rocks, metamorphic decarbonation, and mid-ocean ridge processes [Berner et al., 1983]. The primary source of alkalinity to the oceans is the flux of riverine Ca^{++} and Mg^{++} from the chemical weathering of carbonate and silicate rocks. The primary sink for alkalinity and carbon in the oceans and atmosphere is the formation of sedimentary carbonate rock. Sedimentary carbonate rock accumulates in two principle settings. In shallow water environments, carbonate masses are formed by coral, algae, mollusks, bryozoans, stromatolites, and other neritic organisms. On the seafloor underlying deep water, calcareous sediments have accumulated since the Jurassic, derived from the carbonate tests of pelagic plankton [Wilson, 1975; Boss and Wilkinson, 1991].

Following the Cretaceous/Tertiary (K/T) boundary mass extinction, the per-unit-area rate of deepwater carbonate accumulation rates diminished dramatically [Zachos and Arthur, 1986; Herbert and D'Hondt, 1990; Stott and Kennett, 1990; Rea et al., 1990]. How did this diminution of deepwater carbonate accumulation affect the long-term global carbon cycle?

Postboundary decreases in carbonate accumulation rates were dramatic and widespread. Zachos and Arthur [1986], based on a biostratigraphic analysis of the Deep Sea Drilling Project (DSDP) sites 47.2, 356, 384, and 577, concluded that pelagic carbonate accumulation rates fell from a preboundary value between 0.5 and 2.0 g cm^{-2} kyr^{-1} to a postboundary value between 0.1 and 0.4 g cm^{-2} kyr^{-1}. Characteristic latest Cretaceous pelagic carbonate accumulation rates were about 1 g cm^{-2} kyr^{-1}, and characteristic postboundary accumulation rates were about 0.25 g cm^{-2} kyr^{-1}, suggesting approximately a fourfold reduction in per-unit-area carbonate accumulation across the K/T boundary. Herbert and D'Hondt [1990], using inferred precessional cyclicity in the sediments, estimated an approximate halving of the carbonate accumulation rate across the boundary at DSDP sites 356, 516F, 525A, 527, 528, and 529. Stott and Kennett [1990], based on a biostratigraphic analysis of Ocean Drilling Project (ODP) hole 690C near Antarctica, concluded that carbonate accumulation rates fell from a preboundary value between 1.1 and 1.8 g cm^{-2} kyr^{-1} to a postboundary value of 0.1 to 0.2 g cm^{-2} kyr^{-1} — a greater than

fivefold reduction. In the Indian Ocean at ODP site 752, calculations indicate that carbonate accumulation rates diminished by 90% across the boundary [Rea et al., 1990].

These data present a significant problem in understanding the dynamics of carbonate accumulation. For several million years following the K/T boundary, carbonate accumulation seems to have been in balance with geologic sources of alkalinity and carbon. If there were no mechanism to compensate for the post K/T boundary reduction in deepwater carbonate accumulation per unit area, then oceanic carbon and alkalinity concentrations should have increased, causing a major decrease in atmospheric carbon dioxide content and climatic cooling over this period of time [Caldeira et al., 1990].

If about one third of the Late Cretaceous seafloor was bathed in calcite-saturated waters [Delaney and Boyle, 1988], then a threefold reduction in calcite productivity could be accommodated by a deepening of the calcite lysocline and compensation depth. However, if global pelagic calcite productivity fell by a factor of greater than 3, then there is a problem in removing carbon and alkalinity from the world's oceans.

Opdyke and Wilkinson [1988] estimated that Late Cretaceous deep-ocean carbonate accumulation rates were between 0.05 x 10^6 km^3 yr^{-1} (using estimates from Whitman and Davies [1979]) and 0.25 x 10^6 km^3 yr^{-1} (using a constant accumulation rate) — roughly equivalent to about 1 to 5 x 10^{12} mol $CaCO_3$ yr^{-1}. If the carbonate was accumulating at 1 g cm^{-2} kyr^{-1}, and ~40 x 10^6 km^2 of seafloor were accumulating carbonate sediments [Opdyke and Wilkinson, 1988], then the Late Cretaceous deepwater carbonate accumulation rate was about 4 x 10^{12} mol $CaCO_3$ yr^{-1}. Total latest Cretaceous carbonate accumulation rates are estimated to have been about 20 x 10^{12} mol yr^{-1} [Opdyke and Wilkinson, 1988], suggesting that approximately 20% of the latest Cretaceous carbonate accumulation was in deepwater environments. This contrasts markedly with today's partitioning of carbonate accumulation, in which over 60% of carbonate accumulation occurs in deepwater environments [Wilkinson and Walker, 1989]. If we take 4 x 10^{12} mol $CaCO_3$ yr^{-1} as a representative latest Cretaceous pelagic carbonate flux combined with the estimated 75% reduction in per-unit-area carbonate accumulation in the earliest Tertiary (without

increases in other carbonate sinks or reductions in weathering sources), then approximately 6 x 10^{12} eq yr^{-1} of alkalinity and 3 x 10^{12} mol yr^{-1} of carbon would accumulate in the oceans and atmosphere. An imbalance of this magnitude would push the calcite lysocline to the ocean bottom in ~10^4 years.

THE MODEL

To study the effects that a perturbation of this kind would have on ocean chemistry and atmospheric pCO_2 and to investigate possible geochemical feedbacks that might act to stabilize the Earth's chemistry and climate against this kind of perturbation, we developed a five-box geochemical model of the oceans and atmosphere (Figure 1). This model is of a type first developed and applied to K/T boundary ocean chemistry by Kasting et al. [1986]. That work extended a simple two-box ocean model by including riverine fluxes that are a function of the atmospheric CO_2 concentration and a parameterization for carbonate sedimentation as a function of the deep-ocean carbonate ion concentration. The model developed here represents the atmosphere with a single box and the oceans with four boxes: (1) a surface box representing the oceanic mixed layer, (2) a surface box representing the formation area for deep water, (3) an intermediate-water box representing the pycnocline and the zone in which organic detritus is primarily regenerated, and (4) a deepwater box representing the zone in which detrital pelagic carbonate may dissolve or accumulate in the sediments. For each oceanic box, concentrations of total dissolved inorganic carbon, total dissolved inorganic ^{13}C, total alkalinity, oxygen, and phosphate are calculated. For the atmosphere, only CO_2 and $^{13}CO_2$ concentrations are calculated.

Detrital organic carbon, for the most part, is regenerated in the intermediate waters [Seuss, 1980; Broecker and Peng, 1982]. The flux of organic carbon from the surface to the intermediate waters decreases the intermediate-water carbonate ion concentration. These intermediate waters are generally saturated with respect to calcite; hence, the calcite fraction of this detrital flux passes through the intermediate waters — either to dissolve in the deep ocean or to be preserved in the sediments. Calcite dissolution in the deep ocean increases the deepwater carbonate ion concentration.

Evidence suggests that in the latest Cretaceous, the mean deepwater formation temperature was ~12°C [Savin, 1977; Brass et al., 1982]. Presumably, as in

today's ocean, the pycnoclines of the intermediate waters and deep waters reached the surface near the sites of deepwater formation, allowing the intermediate and deep waters to exchange carbon with the atmosphere without involving mixing through the broad expanse of the ocean mixed layer.

A four-box ocean model is the simplest model that can differentiate the mixed layer, intermediate-water, deep-ocean, and deepwater formation areas. In this model, the mixed layer box represents 90% of the ocean surface and extends to 100 m in depth. The deepwater forming region covers the remaining ocean surface and extends to 400 m in depth. The intermediate-water box lies beneath the mixed layer box and extends to 1500 m depth. The remaining ocean is taken up by the deepwater box.

There is insufficient evidence to completely constrain latest Cretaceous ocean circulation, and it is possible that ocean circulation changed significantly on the 10^5- to 10^6-year time scale modeled here [Schmitz et al., 1992]. Nevertheless, factors such as oxygen utilization and planktonic-benthic $\partial^{13}C$ differences can serve as partial constraints [Berger and Spitzy, 1988]. At DSDP site 577, Upper Maestrichtian $\partial^{13}C$ values from fine fraction samples, reflecting primarily surface ocean conditions, ranged from ~2.5 to ~3‰; benthic values ranged from ~0.2 to ~1.1‰ [Zachos and Arthur, 1986]. At ODP Site 750, Upper Maestrichtian bulk samples yielded $\partial^{13}C$ values of ~2.1‰ , whereas benthic foraminifera yielded $\partial^{13}C$ values of 1.1 to 1.15‰ [Zachos et al., 1992]. Leg 113 values for Maestrichtian planktonic foraminifera range from 2.1 to ~3‰, with benthic values of 1.1 to 1.5‰ before 66.7 Ma, rising to ~2‰ before the boundary (nominally, 66.4 Ma) [Stott and Kennett, 1990]. Most important for this model, preboundary surface-to-deep $\partial^{13}C$ differences were of the order of 1‰ prior to the boundary, and this difference largely collapsed after the boundary [Zachos and Arthur, 1986; Stott and Kennett, 1990].

Although the circulation presented here is not the only possible representation of latest Cretaceous ocean circulation, the pattern is consistent with the $\partial^{13}C$ distribution described above and the inferred generally oxic condition of the deep ocean. The circulation used here (Figure 1) involves a 10-Sv (1 Sverdrup = 10^6 m^3 s^{-1}) mixing between (1) the mixed layer and intermediate waters (denoted F_{mi}), (2) the deepwater forming region and intermediate

waters (F_{wi}), and (3) the deepwater forming region and the deep waters (F_{wd}); a 20-Sv mixing flux between the intermediate and deep waters (F_{id}); and a 10-Sv thermohaline circulation, half of which flows from the deepwater forming region to the intermediate waters and up to the mixed layer (F_i), and half of which enters the deep waters and then flows up through the intermediate waters to the mixed layer (F_d). This ocean circulation pattern, while simplified, demonstrates the fundamental points with regard to carbonate sedimentation and produces carbon isotope and oxygen distributions consistent with the geologic record.

Oxygen

An oxygen mass balance can be written on the assumption that the oxygen concentrations in surface waters are roughly in equilibrium with the overlying atmosphere and that oxygen is consumed in deeper water by the oxidation of detrital organic matter [Broecker and Peng, 1982]. Sediment trap data from the modern ocean [Seuss, 1980] suggest that 97.2% of primary productivity of organic carbon is regenerated by 1500-m depth (the depth of the interface between the intermediate and deep waters in this model). As an approximation, in this model, all primary productivity is regenerated in the intermediate-water box.

In today's oceans there is approximately a four-to-one ratio of organic-to-inorganic carbon productivity [Wenk and Siegenthaler, 1985]. Applying this ratio to the latest Cretaceous, the 1-g $CaCO_3$ cm^{-2} kyr^{-1} productivity estimate suggests latest Cretaceous total biological carbon productivity of ~0.5 mol C m^{-2} yr^{-1}, about half the value estimated by steady state models of today's oceans [Sundquist, 1985]. The use of a higher ratio of organic-to-inorganic carbon productivity would require more rapid ocean mixing to maintain oxygenated intermediate waters, produce sufficient pelagic carbonate accumulation, and maintain observed surface-to-deep $\partial^{13}C$ differences — but these changes would not markedly change the fundamental results.

Late Cretaceous bottom water was about 10°–12°C [Savin, 1977], suggesting an equivalent temperature for the deepwater forming region. The solubility of oxygen in deepwater forming areas at 12°C would be ~0.27 mol O_2 m^{-3}. In today's oceans dissolved O_2 in surface waters between 25° and 30°C scatters around 0.2 mol O_2 m^{-3} [Broecker and Peng, 1982, p.

129]. A steady state O_2 mass balance can be written on intermediate-water oxygen concentration, U_i:

$$C_{m,org} + (F_{mi} + F_{wi} + F_{di} + F_i + F_d)\, U_i = F_{mi}\, U_m + (F_{wi} + F_i)\, U_w + (F_{di} + F_d)\, U_d, \quad (1)$$

and for the deepwater oxygen concentration, U_d:

$$C_{w,org} + (F_{wd} + F_{di} + F_d)\, U_d = (F_{wd} + F_d)\, U_w + F_{di}\, U_i, \quad (2)$$

where $C_{m,org}$ and $C_{w,org}$ are the total organic carbon primary productivity in the mixed layer and deepwater forming regions, respectively, and U_m and U_w are the oxygen concentrations in the oceanic mixed layer and deepwater forming regions, respectively. Because the Late Cretaceous to early Tertiary waters seem to have been largely oxygenated, we infer that the proposed circulation and organic carbon productivity must satisfy the condition that U_i and U_d are both greater than 0 mol O_2 m^{-3}. If the organic C flux was about 0.4 mol m^{-2} yr^{-1} over an area of about 3.3 x 10^{14} m^2 as estimated above, then the proposed circulation meets these criteria with U_i = 0.12 mol O_2 m^{-3} and U_d = 0.17 mol O_2 m^{-3}. Sulfur isotopic evidence for a brief (~70 kyr) anoxic event at the K/T boundary has been reported from Japan [Kajiwara and Kaiho, 1992]; however, this anoxia does not appear to be global in extent.

Phosphate

A phosphate balance for the intermediate waters, deep waters, and the deepwater formation region can be written as

$$(F_{mi} + F_{wi} + F_{di} + F_i + F_d)\, P_i = F_{mi}\, P_m + (F_{wi} + F_i)\, P_w + (F_{di} + F_d)\, P_d + P_{m,org}, \quad (3)$$

$$(F_{wd} + F_{di} + F_d)\, P_d = (F_{wd} + F_d)\, P_w + F_{di}\, P_i + P_{w,org}, \quad (4)$$

$$(F_{wd} + F_{wi} + F_i + F_d)\, P_w + P_{w,org} = (F_i + F_d)\, P_m + F_{wd}\, P_d + F_{wi}\, P_i, \quad (5)$$

where $P_{m,org}$ and $P_{w,org}$ are the biogenic detrital phosphate fluxes from the mixed layer to the intermediate waters and from the deepwater forming region to the deep waters, respectively, and the various P variables represent phosphate concentrations, subscripted as above with oxygen.

If phosphate is limiting mixed layer primary productivity, then mixed layer primary phosphate concentrations will be small when compared to deep-ocean or intermediate-water phosphate concentrations. Therefore, mixed layer phosphate concentration (P_m) can be taken to be approximately zero. This allows the remaining equations to be solved for P_w, P_i and P_d. The solution, using the circulation, the "Redfield" ratio, and the organic carbon productivity described above, is $P_w = 0.8$ mmol PO_4 m^{-3}, $P_i = 1.5$ mmol PO_4 m^{-3}, and $P_d = 1.3$ mmol PO_4 m^{-3}.

Phosphate is used only to develop Late Cretaceous initial conditions for the model, and we do not use phosphate to limit productivity of the early Tertiary "Strangelove ocean" [Hsu and McKenzie, 1990].

Carbon and Alkalinity

The model equations for the distribution of carbon are:

$$V_m \frac{dC_m}{dt} = C_r + C_{m,g} + F_{mi} C_i + (F_{wi} + F_i) C_w + (F_{di} + F_d) C_d - (F_{mi} + F_i + F_d) C_m - C_{m,bio} - C_{sed,shallow}, \quad (6)$$

$$V_i \frac{dC_i}{dt} = F_{mi} C_m + (F_{wi} + F_i) C_w + C_{m,org} + (F_{di} + F_d) C_d - (F_{mi} + F_{wi} + F_{di} + F_i + F_d) C_i, \quad (7)$$

$$V_d \frac{dC_d}{dt} = (F_{wd} + F_d) C_w + F_{di} C_i + C_{w,bio} + C_{m,carb} - ((F_{wd} + F_{di} + F_d) C_d + C_{sed,deep}), \quad (8)$$

$$V_w \frac{dC_w}{dt} = C_{w,g} + (F_i + F_d) C_m + F_{wd} C_d + F_{wi} C_i - ((F_{wd} + F_{wi} + F_i + F_d) C_w + C_{w,bio}), \quad (9)$$

$$M_{atm} \frac{dC_a}{dt} = C_{met} - (C_{w,g} + C_{m,g} + R_{sil} C_r), \quad (10)$$

where V represents the volume of the box denoted by the subscript, and C, when subscripted with an oceanic box subscript (m, w, i or d) represents the concentration of total dissolved carbon in the respective oceanic box. C_a is the atmospheric concentration of CO_2, C_r is the riverine flux of

dissolved inorganic carbon (principally bicarbonate), and $C_{m,g}$ and $C_{w,g}$ are the fluxes of carbon from the atmosphere to the mixed layer and deepwater forming region, respectively. $C_{m,bio}$ and $C_{w,bio}$ represent the total biogenic carbon fluxes from the mixed layer and deepwater forming boxes, respectively. $C_{m,org}$ and $C_{w,org}$ represent the organic carbon fraction of these fluxes, taken to be 0.8 times $C_{m,bio}$ and $C_{w,bio}$, respectively. $C_{m,g}$ and $C_{w,g}$ represent the net CO_2 gas flux from the atmosphere to the surface ocean waters and are calculated as the product of the box area, a gas exchange constant (the value used is that of Wenk and Siegenthaler [1985] for the warm box in their surface ocean), and the difference in CO_2 partial pressure in the surface boxes and atmosphere. The carbonate chemistry in the oceans is calculated using the dissociation constants in Broecker and Peng [1982], without the assumption of negligible concentrations of dissolved CO_2. R_{sil} is the fraction of carbon in the riverine flux derived from atmospheric sources through the weathering of silicate rocks (taken to be 0.32 [Berner et al., 1983]).

The model equations for ^{13}C parallel those for carbon, except that there are certain fractionations of ^{13}C relative to total carbon. The treatment of $\partial^{13}C$ here is comparable to the treatment in Toggweiler and Sarmiento [1985]. Because this model does not include the organic carbon subcycle, to create a Late Cretaceous steady state, the mean $\partial^{13}C$ value of carbon derived from metamorphic, mantle, and carbonate sources must equal the $\partial^{13}C$ of Late Cretaceous carbonate sediments.

The model equations for the distribution of alkalinity are:

$$V_m \frac{d[A_m]}{dt} = A_r + F_{mi} A_i + (F_{wi} + F_i) A_w + (F_{di} + F_d) A_d - (F_{mi} + F_i + F_d) A_m - A_{m,bio} - A_{sed,shallow}, \quad (11)$$

$$V_i \frac{d[A_i]}{dt} = F_{mi} A_m + (F_{wi} + F_i) A_w + (F_{di} + F_d) A_d + A_{m,org} - ((F_{mi} + F_{wi} + F_{di} + F_i + F_d) A_i), \quad (12)$$

$$V_d \frac{d[A_d]}{dt} = (F_{wd} + F_d) A_w + F_{di} A_i + A_{w,bio} + A_{m,carb} - ((F_{wd} + F_{di} + F_d) A_d + A_{sed,deep}), \quad (13)$$

$$V_w \frac{d[A_w]}{dt} = (F_i + F_d) A_m + F_{wd} A_d + F_{wi} A_i - ((F_{wd} + F_{wi} + F_i + F_d) A_w + A_{w,bio}), \quad (14)$$

where the variables parallel the variables described above with the following exceptions: The letter A represents concentrations or fluxes of alkalinity, $A_{m,carb}$ is twice $C_{m,carb}$; $A_{m,org}$ is 17/130 $C_{m,org}$, and $A_{m,bio}$ is $A_{m,carb}$ plus $A_{m,org}$. The calculations for $A_{w,carb}$, $A_{w,org}$ and $A_{w,bio}$ parallel the calculations for $A_{m,carb}$, $A_{m,org}$, and $A_{m,bio}$.

Riverine fluxes of alkalinity (A_r) and bicarbonate (C_r) are parameterized as the product of today's fluxes, as given by Berner et al. [1983], and the weathering rate formulation of Berner [1990], incorporating latest Cretaceous land area and continental position factors. These riverine fluxes are taken to enter the ocean mixed layer box. The flux of calcium carbonate from the mixed layer to shallow-water sediments, $C_{sed,shallow}$, follows a form suggested by Opdyke and Wilkinson [1993]:

$$C_{sed,shallow} = k_s^C (\Omega - 1)^n, \qquad (15)$$

where Ω is the mixed layer aragonite saturation state, computed from the carbonate-ion concentration and temperature of the mixed-layer. In laboratory studies [Burton and Walter, 1987], n has been determined to be about 1.7 at 25°C. Studies of Holocene shallow-water sedimentation rates also suggest a value for n of about 1.7 (B. Opdyke, personal communication, 1992). The value of k_s^C is determined by adjusting this parameter to produce the 80% latest Cretaceous shallow-water carbonate accumulation suggested by the carbonate accumulation data. Because this model ignores the organic carbon subcycle, $A_{sed,shallow}$ is equal to twice $C_{sed,shallow}$.

Equation (15) is empirically supported by relations between Holocene carbonate accumulation rate and saturation state [Opdyke and Wilkinson, 1993]; however, there is a relatively poor mechanistic understanding for this relationship. Photosynthesis often increases the local microscale calcite saturation state, enhancing carbonate precipitation. Nevertheless, even though shallow-water carbonate sediments are predominantly biogenic, a higher ambient saturation state should enhance the biogenic precipitation rate of calcite. On long time scales, however, carbonate accumulation rates are limited by subsidence rates and the areal extent of carbonate accumulation [Opdyke and Wilkinson, 1988]. Hence, if higher shallow-water carbonate-ion concentration were to enhance the long-term

carbonate accumulation rate, it could do so only by expanding the areal extent of carbonate accumulation.

$C_{sed,deep}$ is calculated as a function of deep-ocean carbonate ion concentration as follows:

$$C_{sed,deep} = f_{lys} (C_{w,carb} + C_{m,carb}) , \quad (16)$$

where f_{lys} is a monotonically increasing function of deep-ocean carbonate ion concentration,CO_{3d}. (These values may have been more variable.) The function f_{lys} approaches zero for low values of CO_{3d}, and 1 for high values of CO_{3d}, i.e.,

$$f_{lys} = \frac{1}{2}(1 + \tanh [k_0 (CO_{3d} - k_1)]) . \quad (17)$$

Values for the parameters k_0 and k_1 in equation (7) were computed by taking calcite and aragonite saturation curves from Broecker and Peng [1982], and then computing the fractional sea–floor area above the calcite and aragonite lysoclines using data of Levitus [1982]. These fractional areas were multiplied by the calcite and aragonite fractions in the pelagic detrital carbonate flux, here taken to be 0.5, and then summed. Calcite and aragonite accumulation below their respective lysoclines are ignored. With values for k_0 of 26 mol^{-1} m^3 and for k_1 of 0.11 mol m^{-3}, equation (7) represents an approximation to the detailed calculation for f_{lys} with a maximum difference of less than 0.05 and a root-mean-square difference of less than 0.004.

We ignore dissolution of pelagic sedimentary carbonate as the lysocline shoals, as this would not alter our basic results [Walker and Kasting, 1992] and would substantially complicate the model. In a model without riverine fluxes, the dissolution of pelagic sedimentary carbon has a large effect on atmospheric pCO_2, because carbonate dissolution permits a degree of freedom for the oceanic total alkalinity reservoir. But in our model, the ocean alkalinity reservoir already has this degree of freedom, provided by the alkalinity flux from the dissolution of rocks on land. Walker and Kasting [1992] showed that in an ocean-box model with riverine fluxes, the inclusion of pelagic sedimentary carbonate dissolution has little effect on computed atmospheric CO_2 values.

RESULTS

The model was run using the latest Cretaceous seafloor spreading rate and oceanic plateau

production data from Larson [1991] and the latest Cretaceous land area and geography factors set to 0.93 and 1.27 respectively [Berner, 1990]. The steady state results with (1) pre-K/T boundary pelagic biological fluxes, (2) one-fourth pre-K/T boundary pelagic biological fluxes, and (3) no biological activity are shown in Table 1. The primary result is that in the model, the proposed shallow-water carbonate accumulation formulation of Opdyke and Wilkinson [1993] results in a sufficient increase in shallow-water carbonate accumulation to compensate for complete cessation of pelagic carbonate productivity without the deep ocean becoming fully saturated with respect to calcite. This may explain why the deepest ocean apparently remained unsaturated following the major disruption of pelagic carbonate productivity at the K/T boundary.

In our modeling study, we used the present-day ratio of organic-to-carbonate carbon in the detrital flux. Perhaps, as a result of the extinction of calcareous plankton, there would have been a higher organic-to-carbonate carbon ratio in the detrital flux after the K/T boundary. This would have the effect of increasing surface ocean carbonate-ion concentrations more rapidly than calculated here, permitting the proposed shallow-water carbonate ion/carbon accumulation mechanism to "kick in" earlier than is indicated by this model. Even if the organic-to-carbonate carbon ratio were to diminish, this would affect the timing but not the basic results of the model.

The model was also run in a time-dependent mode, in which all pelagic carbonate and organic carbonate was instantaneously set to zero. While pelagic productivity was not entirely eliminated following the K/T boundary, we reason that if the system is able to buffer the effects of a complete cessation of pelagic productivity, it follows that the system should be able to buffer the effects of a partial cessation. Results of this time-dependent run are shown in Figures 2 through 6.

Figure 2 presents model results of deep-ocean and mixed layer carbonate ion concentration as a function of time after the cessation of pelagic biological productivity. Because the carbonate flux from the mixed layer to the deep ocean is eliminated and because this flux carries more alkalinity than carbon, the very short-term (less than 300 years) effect is to cause a slight reduction in deep-ocean carbonate ion concentration, which causes a slight reduction in the area on which carbonate is accumulating (Figure 3). This is consistent with evidence of the dissolution pulse of carbonate sediments at some sites following the K/T boundary [Zachos and Arthur, 1986].

An understanding of the mixed layer carbonate ion concentration in Figure 2 requires an understanding of the atmospheric pCO_2 results. As the pelagic biological carbon pump is "turned off," CO_2 begins to outgas from the surface ocean, increasing atmospheric CO_2 levels (Figure 4). The elevated atmospheric CO_2 levels cause an increase in the rate of chemical weathering of silicate and carbonate rocks (Figure 5). The elimination of the biological carbon pump also increases mixed layer total dissolved CO_2, causing a decrease in mixed layer carbonate ion concentration on the 10^2- to 10^3-yr time scale. This, according to the parameterization of Opdyke and Wilkinson [1993] would reduce shallow-water carbonate accumulation (Figure 5).

After about 10^3 years, the ocean ceases to outgas, and the influx of riverine alkalinity begins to make the oceans more alkaline, drawing atmospheric CO_2 into the oceans. On the scale of about 10^3 to 10^4 years, the effect of a riverine flux of carbon and alkalinity that is not balanced by marine carbonate accumulation begins to overwhelm the effects of reduced intra-oceanic carbon pumping, and both deep-ocean and mixed layer carbonate ion concentrations begin to rise (Figure 2). The deep-ocean carbonate-ion concentration increases such that approximately 37% of any remaining productivity would dissolve in the deep waters (Figure 3).

Those results are in marked contrast to the results presented in Caldeira et al. [1990], where changes in shallow-water carbonate accumulation were not considered, resulting in saturation of the deep ocean with respect to calcite. This result was contrary to evidence of calcite dissolution at the boundary [J.C. Zachos, personal communication, 1992]. In the present model runs, the carbonate ion concentrations of the mixed layer and deep ocean stabilize within about 20 kyr, because by this time the shallow-water carbonate ion concentration has increased sufficiently to cause an increase in shallow-water carbonate accumulation. This increase in shallow-water carbonate accumulation would compensate for the absence of deepwater carbonate accumulation (Figure 5).

In Figure 4b, various slopes can be seen in the plot of atmospheric pCO_2 against the log of time. The period from 10^0 to 10^3 years after the boundary event represents an outgassing of CO_2 to the atmosphere related to the fact that the deep ocean, without pelagic productivity to maintain strong carbon and alkalinity gradients, effectively comes in contact with the atmosphere, to which it degasses carbon. From about

10^3 to 10^4 years after the boundary event, after cessation of carbonate productivity, a decrease in atmospheric pCO_2 takes place, which is associated with the buildup of alkalinity in the oceans, resulting from the imbalance in riverine and carbonate sedimentation fluxes. These changes in atmospheric CO_2 could have contributed to the brief warming and subsequent cooling reported by Smit [1990] over the first few thousand years following the K/T event. From approximately 10^4 to 10^5 years after carbonate productivity cessation, the atmospheric CO_2 content continues to diminish. During this time, shallow-water carbonate sedimentation exceeds the riverine flux of carbon and alkalinity, removing "excess" carbon and alkalinity from the ocean (Figure 5). Between about 10^5 and 10^6 years after the event, carbonate sedimentation regains balance with chemical weathering, and the atmospheric CO_2 content decays with a time constant of ~3 x 10^5 years. After 10^6 years, the system has effectively reached steady state, and the atmospheric CO_2 level no longer appreciably decays.

Within about 10^3 years after the cessation of pelagic productivity, the mixed layer approaches the deep-ocean carbon-isotopic value (Figure 6), and then, from about 10^3 to 10^6 yr after the productivity turnoff, the deep-ocean and mixed layer carbon isotopic signals move toward the preperturbed mixed layer value. Kump [1991], in a study of "Strangelove ocean" conditions, found similar isotopic behavior using a somewhat simpler model. In less than 10^6 years, the system has approached a new steady state, and the isotopic composition of accumulating sedimentary carbonate, neglecting effects of organic carbon burial [Kump, 1991], once again equals the precessation value.

Based on our CO_2 estimates (Figure 4b), our model predicts a several-degree warming after the boundary, persisting on the 10^3- to 10^4-year time scale. A direct comparison of our model results with evidence of climatic change at the K/T boundary remains difficult, because this evidence indicates both warming and cooling on various time scales [e.g., Schmitz et al., 1992; Rampino, 1993]. Floral analyses in western North America have been interpreted as indicating a brief cooling (possibly an "impact winter") and a longer-term (500 kyr to 1 m.y.) warming of up to 10°C [Wolfe, 1990]. In a very detailed study, Smit [1990] found evidence for an 8°C ocean surface warming at Caravaca and Agost, Spain, in the first few thousand years of the Tertiary.

The analysis of deep-ocean $\partial^{18}O$ data by Zachos and Arthur [1986] indicated no major prolonged warming or cooling trend. Interpretation of these records is made more difficult because some sections may contain unrecognized hiatuses [MacLeod and Keller, 1991].

In this model, if the biological pump is turned back on, the system returns to the pre-K/T boundary state within about 10 kyr. If productivity is turned on as a step function, atmospheric CO_2 diminishes by about one-third for several thousand years; however, the gradual return of biological productivity over tens of thousands of years has little effect on atmospheric CO_2 content.

DISCUSSION AND CONCLUSIONS

This modeling study has shed light on several questions that are important for the understanding of the carbon cycle and events following the mass extinction at the K/T boundary. In the aftermath of the K/T boundary event, pelagic carbonate productivity was sharply reduced, yet the carbon cycle seems to have maintained a general balance between weathering and sedimentation fluxes over the first few hundred thousand years of the Tertiary. If pelagic carbonate productivity diminished by less than a factor of 3 [Herbert and D'Hondt, 1990], then a deepening of the calcite compensation depth could have compensated for the diminished vertical accumulation rates. However, if carbonate productivity diminished by a factor of greater than 3 [Zachos and Arthur, 1986; Stott and Kennett, 1990; Rea et al., 1990], then another mechanism (e.g., carbonate ion control of shallow-water carbonate accumulation) must be invoked to explain why the deep ocean did not become fully saturated with respect to calcite.

Based on model results, shallow-water carbonate accumulation would have had to increase by less than 25% to compensate for the reduction in deepwater carbonate productivity seen at the K/T boundary. While the number of well-studied shallow-water sites is still insufficient to compile an independent carbonate budget for the earliest Tertiary, evidence suggests that post-K/T boundary shallow-water carbonate percentages may have increased at some sites [Barrera and Keller, 1990; Jones et al., 1987], although this could be a result of decreases in noncarbonate sedimentary fluxes. Nevertheless, this may indicate that increases in shallow-water carbonate accumulation might have helped compensate for decreases in deepwater carbonate

accumulation following the K/T boundary extinction of pelagic carbonate-secreting organisms.

It is unclear whether vertical carbonate accumulation rates diminished by a factor of greater than 3 during the so-called "Strangelove ocean" period. However, evidence from sediments in ophiolites, summarized by Boss and Wilkinson [1991], indicates that pelagic carbonate accumulation may have been quite low prior to the evolutionary radiation of pelagic calcareous plankton in the Jurassic. The model developed here demonstrates that the proposed relationship between carbonate ion concentration and shallow-water carbonate accumulation rates [Opdyke and Wilkinson, 1993] could produce sufficient carbonate accumulation to balance riverine inputs, even in a pre-Jurassic ocean largely devoid of deepwater carbonate sedimentation.

Acknowledgements. We thank J.C. Zachos and B.N. Opdyke for helpful reviews and comments. K.C. was supported by an NSF Earth Sciences Postdoctoral Fellowship awarded in 1991. M.R.R. was supported by NASA Grant NAGW-1697.

REFERENCES

Barrera, E., and G. Keller, Stable isotopic evidence for gradual environmental changes and species survivorship across the Cretaceous/Tertiary boundary, *Paleoceanography, 5,* 867–890, 1990.

Berger, W.H., and A. Spitzy, History of atmospheric CO_2: Constraints for the deep-sea record, *Paleoceanography, 3,* 401–411, 1988.

Berner, R. A., Atmospheric carbon dioxide levels of Phanerozoic time, *Science, 249,* 1382–1386, 1990.

Berner, R.A., A.C. Lasaga and R.M. Garrels, The carbonate-silicate geochemical cycle and its effect on atmospheric carbon dioxide over the past 100 million years, *Am. J. Sci., 283,* 641–683, 1983.

Boss, S.K., and B.H. Wilkinson, Planktogenic/eustatic control of cratonic/oceanic carbonate accumulation, *J. Geol., 99*, 497–513, 1991.

Brass, G.W., J.R. Southam and W.H. Peterson, Warm saline bottom water in the ancient ocean, *Nature, 296,* 620–623, 1982.

Broecker, W.S., and T.-H. Peng, *Tracers in the Sea*, Eldigio, Palisades, N. Y., 1982.

Burton, E.A., and L.M. Walter, Relative precipitation rates of aragonite and Mg calcite from seawater: temperature or carbonate ion control? *Geology, 15,* 111–114, 1987.

Caldeira, K., M.R. Rampino, T. Volk and J.C. Zachos, Biogeochemical modeling at mass extinction boundaries: Atmospheric carbon dioxide and ocean alkalinity at the K/T boundary, in *Global Bioevents: Abrupt Changes in the Global Biota Through Time,* edited by E.G. Kauffman and O.H. Walliser, pp. 333–345, Springer-Verlag, New York, 333–345, 1990.

Delaney, M.L., and E.A. Boyle, Tertiary paleoceanic chemical variability: Unintended consequences of simple geochemical models, *Paleoceanography, 3*, 127–156, 1988.

Herbert, T.D., and S.L. D'Hondt, Precessional climate cyclicity in Late Cretaceous-Early Tertiary marine sediments: A high resolution chronometer of Cretaceous-Tertiary boundary events, *Earth Planet. Sci. Lett., 99*, 263–275, 1990.

Hsu, K.J., and J.A. McKenzie, Carbon-isotope anomalies at era boundaries: Global catastrophes and their ultimate cause, *Geol. Soc. Am. Spec. Pap., 247*, 61–70, 1990.

Jones, D.S., et al., Biotic, geochemical and paleomagnetic changes across the Cretaceous/Tertiary boundary at Braggs, Alabama, *Geology, 15,* 311–315, 1987.

Kajiwara, Y., and K. Kaiho, Oceanic anoxia at the Cretaceous/Tertiary boundary supported by the sulfur isotopic record, *Palaeogeogr. Palaeoclimatol. Palaeoecol., 99*, 151–162, 1992.

Kasting, J.F., S.M. Richardson, J.B. Pollack and O.B. Toon, A hybrid model of the CO_2 geochemical cycle and its application to large impact events, *Am. J. Sci., 286,* 361–389, 1986.

Kump, L.R., Interpreting carbon-isotope excursions: Strangelove oceans, *Geology, 19,* 299–302, 1991.

Larson, R. L., The latest pulse of the Earth: Evidence for a mid-Cretaceous super plume, *Geology, 19*, 547–550, 1991.

Levitus, S., Climatological atlas of the world ocean, *NOAA Prof. Pap. 13,* U. S. Govt. Print. Off., Washington D. C., 1982.

Macleod, N., and G. Keller, How complete are Cretaceous/Tertiary boundary sections? A chronostratigraphic estimate based on graphic correlation, *Geol. Soc. Am. Bull., 103*, 1439–1457, 1991.

Opdyke, B.N., and B.H. Wilkinson, Surface area control of shallow cratonic and deep marine carbonate accumulation, *Paleoceanography, 3,* 685–703, 1988.

Opdyke, B.N., and B.H. Wilkinson, Carbonate mineral saturation state and cratonic limestone accumulation, *Am. J. Sci., 293*, 217–234, 1993.

Rampino, M.R., Catastrophe: Comet or asteroid impact, in *Future Climates of the World,* edited by A. Henderson-Sellers, Elsevier, New York, in press, 1993.
Rea, D.K., J. Dehn, N.W. Driscoll, T.R. Janacek, R.N. Owen, J.J. Pospichal, P. Resiwati, and Ocean Drilling Project Leg 121 Scientific Party, Paleoceanography of the eastern Indian Ocean from ODP Leg 121 on Broken Ridge, *Geol. Soc. Am. Bull., 102,* 679–690, 1990.
Savin, S.M., The history of the Earth's surface temperature during the past 100 million years, *Annu. Rev. of Earth Planet. Sci., 5,* 319–355, 1977.
Schmitz, B., G. Keller, and O. Stenvall, Stable isotope and foraminiferal changes across the Cretaceous-Tertiary boundary at Stevns Klint, Denmark: Arguments for long-term oceanic instability before and after bolide-impact event, *Palaeogeogr. Palaeoclimatol. Palaeoecol., 96*, 233–260, 1992.
Seuss, E., Particulate organic carbon flux in the oceans — surface productivity and oxygen utilization, *Nature, 288,* 260–263, 1980.
Smit, J., Meteorite impact, extinctions and the Cretaceous-Tertiary boundary, *Geologie en Mijnbouw, 69*, 187–204, 1990.
Stott, L.D., and J.P. Kennett, The paleoceanographic and paleoclimatic signature of the Cretaceous/Paleogene boundary in the Antarctic: Stable isotopic results from ODP Leg 113, *Proc. Ocean Drill. Program: Sci. Results, 113*, 829–846, 1990.
Sundquist, E.T., Geological perspectives on carbon dioxide and the carbon cycle, in *The Carbon Cycle and Atmospheric CO_2: Natural Variations Archean to Present, (Geophys. Monogr. Ser., vol. 32),* edited by E.T. Sundquist and W.S. Broecker, pp. 5–59, AGU, Washington, D. C., 1985.
Toggweiler, J.R., and J.L. Sarmiento, in *The Carbon Cycle and Atmospheric CO_2: Natural Variations Archean to Present, (Geophys. Monogr. Ser., vol. 32),* edited by E.T. Sundquist and W.S. Broecker, pp. 163–184, AGU, Washington, D.C., 1985.
Walker, J.C.G., and J.F. Kasting, Effect of fuel and forest conservation on future levels of atmospheric carbon dioxide, *Palaeogeogr. Palaeoclimatol. Palaeoecol., 97*, 151–189, 1992.
Wenk, T., and U. Siegenthaler, The high latitude ocean as a control of atmospheric CO_2, in *The Carbon Cycle and Atmospheric CO_2: Natural Variations Archean to Present, (Geophys. Monogr. Ser., vol. 32),* edited by E.T. Sundquist

and W.S. Broecker, pp. 185–194, AGU, Washington, D.C., 1985.
Whitman, J.M., and T.A. Davies, Cenozoic oceanic sedimentation rates — How good are the data? *Mar. Geol., 30,* 269–284, 1979.
Wilkinson, B.H., and J.G.C. Walker, Phanerozoic cycling of sedimentary carbonate, *Am. J. Sci., 289*, p. 525–548, 1989.
Wilson, J.L., *Carbonate Facies in Geologic History,* Springer-Verlag, New York, 1975.
Wolfe, J.A., Paleobotanical evidence for a marked temperature increase following the Cretaceous/Tertiary boundary, *Nature, 343,* 153–156, 1990.
Zachos, J.C., and M.A. Arthur, Paleoceanography of the Cretaceous/Tertiary boundary event: Inferences from stable isotopic and other data, *Paleoceanography, 1*, 5–26, 1986.
Zachos, J.C., M.-P. Aubry, W.A. Berggren, T. Ehrendorfer, F. Heider, and K.C. Lohmann, Chemobiostratigraphy of the Cretaceous/Paleocene boundary at Site 750, southern Kerguelen plateau, *Proc. Ocean Drill. Program, Sci. Results, 120*, 961–974, 1992.

K. Caldeira, Earth System Science Center, Pennsylvania State University, 248 Deike Building, University Park, PA 16802.
M. R. Rampino, Department of Earth System Science, New York University, 34 Stuyvesant Street, New York, NY 10003.

(Received June 25, 1992;
revised April 12, 1993;
accepted April 24, 1993.)

[1]Now at: Global Climate Research Division, Lawrence Livermore National Laboratory, Livermore, CA 94551.

Paper number 93 PA01163.
0883-8305/93/93PA-01163$10.00

Caldeira and Rampino: End-Cretaceous Biogeochemical Stabilization

Caldeira and Rampino: End-Cretaceous Biogeochemical Stabilization

Caldeira and Rampino: End-Cretaceous Biogeochemical Stabilization

Caldeira and Rampino: End-Cretaceous Biogeochemical Stabilization

Caldeira and Rampino: End-Cretaceous Biogeochemical Stabilization

Caldeira and Rampino: End-Cretaceous Biogeochemical Stabilization

Caldeira and Rampino: End-Cretaceous Biogeochemical Stabilization

Caldeira and Rampino: End-Cretaceous Biogeochemical Stabilization

Caldeira and Rampino: End-Cretaceous Biogeochemical Stabilization

Caldeira and Rampino: End-Cretaceous Biogeochemical Stabilization

Fig. 1. Schematic diagram of the model described in the text. Fluid fluxes are shown in heavy arrows with the flux specified in sverdrups (Sv). Biogenic detrital fluxes are shown in heavy dashed arrows. Gas phase carbon dioxide fluxes are shown in thin solid arrows, and sedimentary and weathering carbon and alkainity fluxes are shown in thin dashed arrows.

Fig. 2. Model results for carbonate ion concentration as a function of time. Note that the horizontal time axis is drawn in a logarithmic scale.

Fig. 3. Model results for effective fractional area of the deep seafloor accumulating carbonate (variable f_{lys}, described in text). This variable is computed based on deep-ocean carbonate ion concentration as a function of time, ocean hypsometry, the saturation constant for calcite and aragonite as a function of pressure, and the estimation of the fraction of carbonate productivity that is calcite productivity. Note that the horizontal time axis is drawn in a logarithmic scale.

Fig. 4. Model results for atmospheric pCO_2 as a function of time. (a) Time is shown on a linear scale, and (b) time is shown on a logarithmic scale.

Fig. 5. Model results for the riverine flux of carbon associated with the chemical weathering of carbonate and silicate rocks (C_r), and the flux of shallow-water carbonate sedimentation ($C_{sed,shallow}$). Note that the horizontal time axis is drawn in a logarithmic scale.

Fig. 6. Model results for mixed layer and deep-ocean $\partial^{13}C$. Note that the horizontal time axis is drawn in a logarithmic scale.

TABLE 1. Steady State Results

Parameter	Pelagic Biological Fluxes		
	Full	1/4	None
Percentage of Pre-K/T Boundary Productivity	100	25	0
$C_{sed,deep}$, 10^{12} mol yr^{-1}	5.3	3.4	0.0
$C_{sed,shallow}$, 10^{12} mol yr^{-1}	18.6	20.5	23.9
C_r, 10^{12} mol yr^{-1}	23.9	23.9	23.9
CO_{3m}, mol m^{-2} yr^{-1}	0.16	0.17	0.18
CO_{3d}, mol m^{-2} yr^{-1}	0.08	0.10	0.12
f_{lys}	0.15	0.39	0.63
C_a, ppm	363	363	363
C_m, mol m^{-3}	1.68	1.71	1.76
C_w, mol m^{-3}	1.79	1.79	1.83
C_i, mol m^{-3}	1.90	1.80	1.82
C_d, mol m^{-3}	1.88	1.80	1.82
$\partial^{13}C_a$, $^o/_{oo}$	–4.37	–4.32	–4.30
$\partial^{13}C_m$, $^o/_{oo}$	2.52	2.50	2.50
$\partial^{13}C_w$, $^o/_{oo}$	1.79	2.30	2.51
$\partial^{13}C_i$, $^o/_{oo}$	0.40	1.97	2.50
$\partial^{13}C_d$, $^o/_{oo}$	1.02	2.14	2.50
A_m, eq m^{-3}	1.83	1.87	1.93
A_w, eq m^{-3}	1.88	1.87	1.93
A_i, eq m^{-3}	1.88	1.87	1.93
A_d, eq m^{-3}	1.93	1.88	1.93
$C_{m,org}$, mol m^{-2} yr^{-1}	0.4	0.1	0.0
$C_{w,org}$, mol m^{-2} yr^{-1}	0.4	0.1	0.0
$C_{m,carb}$, mol m^{-2} yr^{-1}	0.1	0.025	0.0
$C_{w,carb}$, mol m^{-2} yr^{-1}	0.1	0.025	0.0

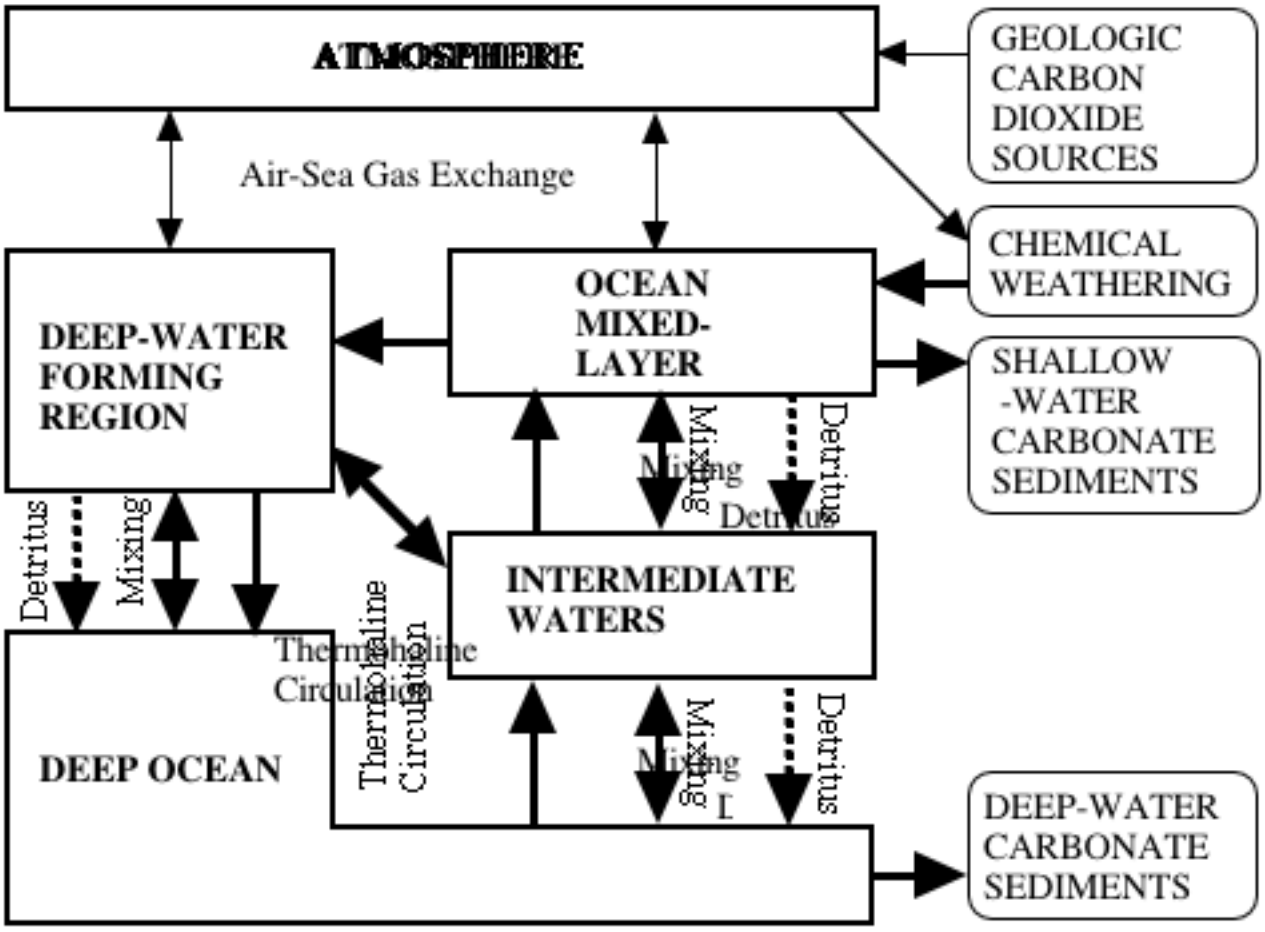
ATMOSPHERE
GEOLOGIC CARBON DIOXIDE SOURCES
Air-Sea Gas Exchange
CHEMICAL WEATHERING
DEEP-WATER FORMING REGION
OCEAN MIXED-LAYER
SHALLOW -WATER CARBONATE SEDIMENTS
Detritus
Mixing
INTERMEDIATE WATERS
Thermohaline Circulation
DEEP OCEAN
DEEP-WATER CARBONATE SEDIMENTS

Figure 1.

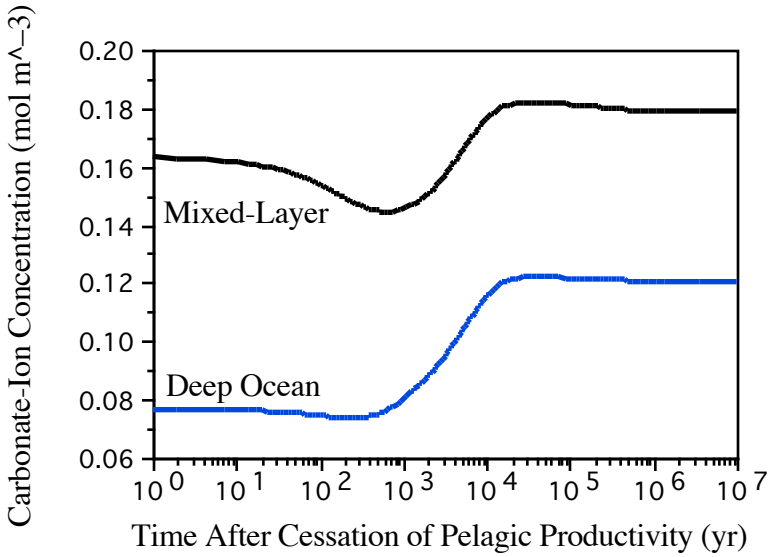

Figure 2. Caldeira and Rampino MS#93PA01163

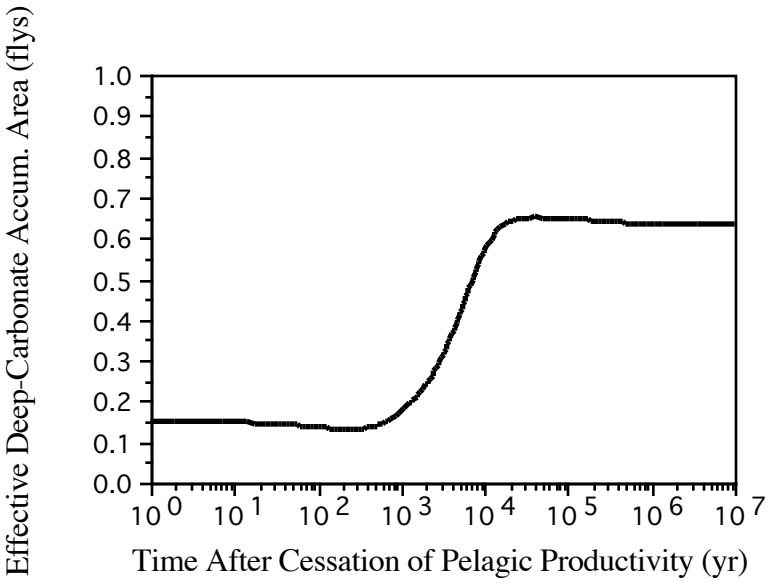

Figure 3. Caldeira and Rampino MS#93PA01163

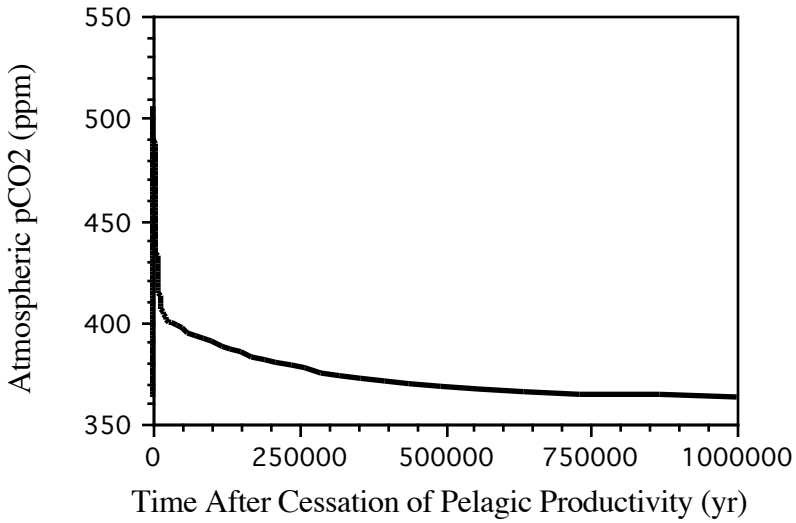

Figure 4a. Caldeira and Rampino MS#93PA01163

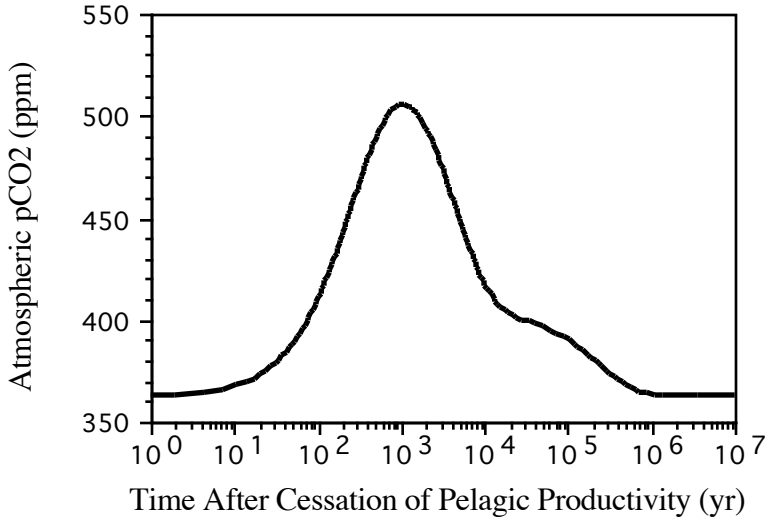

Figure 4b. Caldeira and Rampino MS#93PA01163

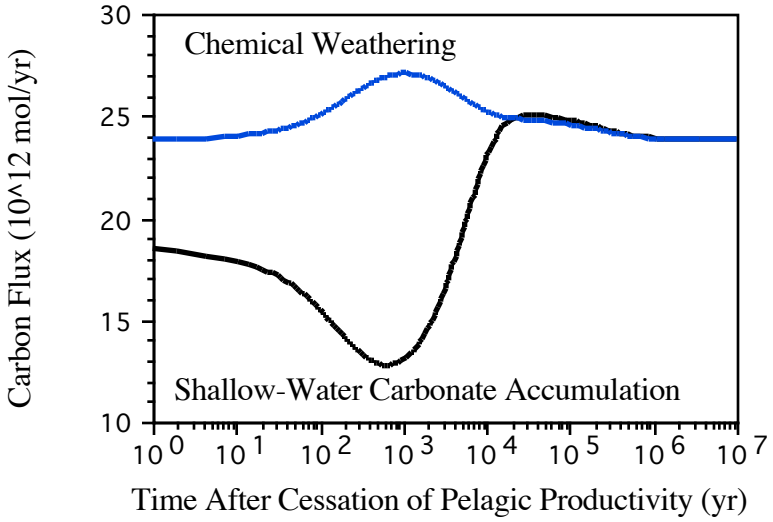

Figure 5. Caldeira and Rampino MS#93PA01163

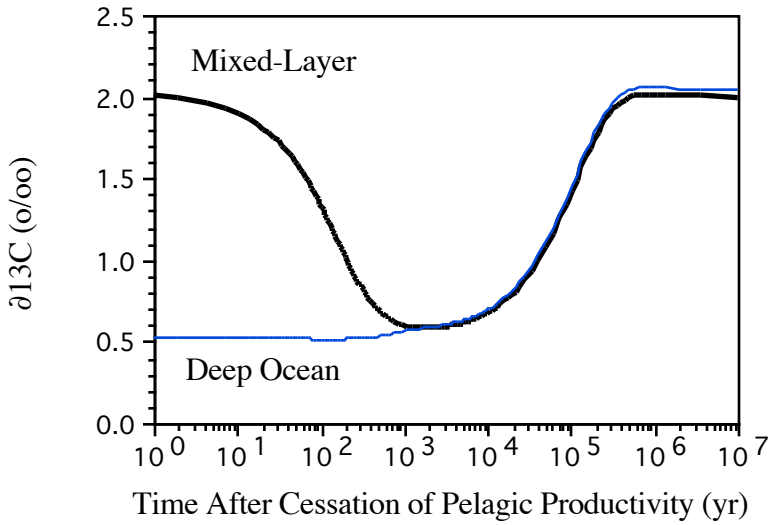

Figure 6. Caldeira and Rampino MS#93PA01163